



Impaired proliferation and migration of HUVEC and melanoma cells by human anti-FGF2 mAbs derived from a murine hybridoma by guided selection

Carolina Georg Magalhães, Carla Ploeger Mansueli, Tânia Maria Manieri, Wagner Quintilio, Angélica Garbuio, Juan de Jesus Marinho, Jane Zveiter de Moraes, Lilian Rumi Tsuruta & Ana Maria Moro

To cite this article: Carolina Georg Magalhães, Carla Ploeger Mansueli, Tânia Maria Manieri, Wagner Quintilio, Angélica Garbuio, Juan de Jesus Marinho, Jane Zveiter de Moraes, Lilian Rumi Tsuruta & Ana Maria Moro (2023) Impaired proliferation and migration of HUVEC and melanoma cells by human anti-FGF2 mAbs derived from a murine hybridoma by guided selection, *Bioengineered*, 14:1, 2252667, DOI: [10.1080/21655979.2023.2252667](https://doi.org/10.1080/21655979.2023.2252667)

To link to this article: <https://doi.org/10.1080/21655979.2023.2252667>



© 2023 The Author(s). Published by Informa UK Limited, trading as Taylor & Francis Group.



[View supplementary material](#)



Published online: 04 Sep 2023.



[Submit your article to this journal](#)



Article views: 195







[View related articles](#)



[View Crossmark data](#)

Impaired proliferation and migration of HUVEC and melanoma cells by human anti-FGF2 mAbs derived from a murine hybridoma by guided selection

Carolina Georg Magalhães ^a, Carla Ploeger Mansueli^a, Tânia Maria Manieri^a, Wagner Quintilio^a, Angélica Garbuio^a, Juan de Jesus Marinho^a, Jane Zveiter de Moraes ^b, Lilian Rumi Tsuruta ^a, and Ana Maria Moro ^{a,c}

^aLaboratory of Biopharmaceuticals, Butantan Institute, São Paulo, Brazil; ^bDepartment of Biophysics, Escola Paulista de Medicina, Universidade Federal de São Paulo, São Paulo, Brazil; ^cCeRDI, Center for Research and Development in Immunobiologicals, Butantan Institute, São Paulo, Brazil

ABSTRACT

Disadvantages of using murine monoclonal antibodies (mAb) in human therapy, such as immunogenicity response, led to the development of technologies to transform murine antibodies into human antibodies. The murine anti-FGF2 3F12E7 mAb was proposed as a promising agent to treat metastatic melanoma tumors; once it blocks the FGF2, responsible for playing a role in tumor growth, angiogenesis, and metastasis. Considering the therapeutic potential of anti-FGF2 3F12E7 mAb and its limited use in humans due to its origin, we used this antibody as the template for a guided selection humanization technique to obtain human anti-FGF2 mAbs. Three Fab libraries (murine, hybrid, and human) were constructed for humanization. The libraries were phage-displayed, and the panning was performed against recombinant human FGF2 (rFGF2). The selected human variable light and heavy chains were cloned into AbVec vectors for full-length IgG expression into HEK293-F cells. Surface plasmon resonance analyses showed binding to rFGF2 of seven mAbs out of 20 expressed. Assays performed with these mAbs resulted in two that showed proliferation reduction and cell migration attenuation of HUVEC and SK-Mel-28 melanoma cells. In-silico analyses predicted that these two human anti-FGF2 mAbs interact with FGF2 at a similar patch of residues than the chimeric anti-FGF2 antibody, comprehending a region within the heparin-binding domains of FGF2, essential for its function. These results are comparable to those achieved by the murine anti-FGF2 3F12E7 mAb and showed success in the humanization process and selection of two human mAbs with the potential to inhibit undesirable FGF2 roles.

HIGHLIGHTS

- The guided selection humanization process enabled the production of 20 human mAbs anti-FGF2;
- Seven human anti-FGF2 mAbs showed binding to the rFGF2 antigen in the SPR binding assay;
- Two human anti-FGF2 mAbs inhibited the proliferation and migration of HUVEC and SK-Mel-28 cells and were predicted to contact the FGF2 at a similar patch of residues than the original mAb.

ARTICLE HISTORY

Received 8 February 2023
Revised 23 May 2023
Accepted 25 May 2023

KEYWORDS

Antibody humanization; fibroblast growth factor 2; fragment antigen-binding; guided selection; phage display


Introduction

Hybridoma technology introduced in 1975 proved to be an efficient method to generate murine monoclonal antibodies (mAb) [1], and about 10 years later, a murine anti-CD3 mAb (Muromonab – Orthoclone

OKT3) was the first therapeutic antibody approved by FDA [2]. However, despite the success of the hybridoma technology in selecting mAbs with high affinity and specificity, there are limitations to the use of non-human antibodies for therapeutic application due to

CONTACT Ana Maria Moro  ana.moro@butantan.gov.br  Laboratory of Biopharmaceuticals, Butantan Institute, São Paulo, Brazil

[#]Graduate Immunology Program, University of São Paulo. Present affiliation: 1. Rutgers Cancer Institute of New Jersey, Newark, NJ 07101, USA; 2. Division of Cancer Biology, Department of Radiation Oncology, Rutgers New Jersey Medical School, Newark, NJ 07103, USA.

 Supplemental data for this article can be accessed online at <https://doi.org/10.1080/21655979.2023.2252667>

© 2023 The Author(s). Published by Informa UK Limited, trading as Taylor & Francis Group.

This is an Open Access article distributed under the terms of the Creative Commons Attribution-NonCommercial License (<http://creativecommons.org/licenses/by-nc/4.0/>), which permits unrestricted non-commercial use, distribution, and reproduction in any medium, provided the original work is properly cited. The terms on which this article has been published allow the posting of the Accepted Manuscript in a repository by the author(s) or with their consent.

the induction of an immunogenic response [3] and adverse effects [4] resulting in loss of efficacy and poor pharmacokinetic profiles [5].

In the past years, significant advances in antibody humanization technologies, together with new methods to generate human antibodies, have been effective as alternatives to obtaining therapeutic antibodies [6], and, to date, more than 120 antibodies have been approved by the FDA and/or EMA [7]. Historically, the first approach to engineering the antibodies and reducing their murine content resulted in chimeric antibodies with the murine antibody constant domains replaced by human homologs (approximately 70% of human content) [8]. This technique allows decreased immunogenicity of the antibodies and preservation of the murine parental antibody specificity. However, murine variable domains can still induce the production of human anti-chimeric antibodies (HACA) in approximately 40% of patients treated with chimeric antibodies [3]. To further reduce the murine content, humanized antibodies were generated [9], and the complementarity-determining regions (CDR) grafting method was the first humanization technique developed [10]. In this technique, the murine sequences of the CDRs, which mediate most of the interaction with the antigen, are grafted into a human framework. It is one of the most used antibody humanization techniques; however, despite the initial success of the CDR grafting method, most of the antibodies produced by this technique showed a reduction in antigen binding affinity compared to the murine parental antibody, requiring back mutations for the maintenance of some murine amino acids in the framework to stabilize the antibody binding structure [11,12].

Several other antibody humanization methods were developed, focusing on the construction of variants based on the murine antibody structure and sequence analysis, substituting exposed residues on the surface of the antibodies (veneering) [13], and selecting clones from combinatorial libraries [14]. Combinatorial human antibody libraries are constructed by amplifying light (LC) and heavy (HC) chain genes from peripheral blood lymphocytes, lymph nodes, spleen, or bone marrow [15] antibody fragments specific to a given molecule can be performed using *in vitro* display

technologies. The phage display technology was the first *in vitro* display platform developed by presenting an exogenous peptide on the surface of a filamentous bacteriophage (phage) [16] and allows the selection of a fully human antibody through entirely *in vitro* processes, independent of the *in vivo* immune response; and, obtaining mAbs against any antigen such as self-antigens, toxic, unstable, and non-immunogenic [17]. Guided selection by phage display is a method to obtain a fully human antibody using combinatorial libraries by replacing the immunoglobulin genes of any non-human parental antibody, which serves as a template, with human immunoglobulin genes using a human antibody library [18–24]. This technique was used to generate the first fully human antibody approved by the FDA in 2002, the anti-TNF- α Humira (adalimumab) [19]. It is a practical methodology for humanizing antibody candidates with desired biological activity once it allows the selection of fully human antibodies and uses the target antigen in all selection steps to obtain clones with affinity to the target [22].

In this work, we used the murine anti-FGF2 3F12E7 mAb generated by hybridoma technology as a template for humanization through the guided selection technique. The parental murine mAb showed promising antitumor activity in strategic experimental approaches, decreasing the vascular tumor density and inhibiting tumor growth and metastasis [25]. This antibody targets the fibroblast growth factor 2 (FGF2), one of the first angiogenic factors identified [26,27], that, besides being enrolled in the regulation of angiogenesis, can act as an oncogenic factor inducing tumor cell proliferation and playing an essential role in cancer progression [28–30]. The overexpression of FGF2, and excessive mitogenic FGF2/FGFR signaling, are associated with aggressive cancer phenotypes, correlate with poor prognosis, and induce tumor angiogenesis, development of disorganized vasculature, tumor growth, and metastases [28–33].

Considering the importance of FGF2 in tumor progression and the limited therapeutic use of the murine anti-FGF2 3F12E7 mAb in humans, we used the sequential guided selection approach to obtain human antibodies corresponding to the murine anti-FGF2 3F12E7 mAb. Since hybridomas have been shown to often contain multiple functional

and nonfunctional variable region genes [34,35], a murine Fab library was first created from the 3F12E7 hybridoma and screened for recombinant human FGF2 (rFGF2) binders. The lead Fab binder was then used to create a hybrid human/murine Fab library, and finally, the human library, all selected against the rFGF2. Then, from the human antibodies panel, we set two of them with properties of proliferation reduction and migration attenuation of human endothelial cells (HUVEC) and human melanoma cells (SK-Mel-28), with similar results obtained *in vitro* with the murine anti-FGF2 3F12E7 mAb.

Materials and methods

Mammalian cell culture

3F12E7 hybridoma cells secreting murine anti-FGF2 mAb [25] were cultured in RPMI-1640 medium (Thermo Fisher Scientific, Catalog No. 11875119) with 10% fetal bovine serum (FBS) (Cultilab, Catalog No. F063) and 4 mM L-glutamine (Sigma-Aldrich, Catalog No. G2150). Human Umbilical Vein Endothelial Cell (HUVEC) (Lonza, Catalog No. CC-2519) were grown in EBM-2 medium (Lonza, Catalog No. CC-3156) supplemented with the EGM-2 kit (Lonza, Catalog No. CC-4147). Human melanoma cells SK-Mel-28 (ATCC, HTB-72) were grown in DME-F12 medium (Sigma-Aldrich, Catalog No. D6421) with 10% FBS. These cells were maintained at 37°C in 5% CO₂. FreeStyle™ 293-F HEK cells (Thermo Fisher Scientific, Catalog No. R790-07) were cultured in FreeStyle™ 293F medium (Thermo Fisher Scientific, Catalog No. 12338-018) and maintained at 37°C with constant stirring at 120 rpm and 8% CO₂.

Construction of LC and Fd human libraries

LC and Fd (VH and first constant domain of the HC) genes were amplified from cDNA pools obtained from PBMC of 100 healthy donors according to previously described [15,36]. All donors signed informed consent forms by the Human Ethics Committee of the Brazil Platform (CAAE n° 43930115.6.0000.5467). The human LC naïve library containing the repertoire of kappa and lambda families and the human Fd naïve library were both constructed in the pComb3X

vector [15]. The size of each naïve library (LC or Fd) is 10 [7] clones.

Construction of combinatorial fragment antigen-binding (Fab) libraries

Murine Fab library

The total RNA of 3F12E7 hybridoma cells was extracted with TRIzol (Thermo Fisher Scientific, Catalog No. 15596026). The cDNA was synthesized using the SuperScript™ First-Strand Synthesis System for RT-PCR (Thermo Fisher Scientific, Catalog No. 11904018). Immunoglobulin LC and Fd genes were amplified using specific primers for murine immunoglobulins based on the Kabat database [37]. The primers contain specific restriction sites (*SacI* and *XbaI* for the LC gene and *XhoI* and *SpeI* for the Fd gene) for cloning in the pComb3X vector [15], licensed from The Scripps Research Institute. The PCR amplification was conducted in 50 µL, containing 0.8 mM dNTPs, 1.25 U *Taq* DNA polymerase (Thermo Fisher Scientific, Catalog No. 10342178), 1.5 mM MgCl₂, PCR Buffer 1× (Thermo Fisher Scientific, Catalog No. 10342178), 0.4 µM each primer and 2 µL cDNA. The cycling conditions were: initial melt at 94°C for 1 min followed by 40 cycles of a three-step program (94°C, 1 min; 57°C, 1 min; 72°C, 1 min) and extension step at 72°C for 5 min. The PCR products were analyzed through 1.5% agarose gel, and the LC (or Fd) genes were concentrated and purified by ethanol precipitation to obtain the repertoire of LC and Fd genes. The murine LC and Fd genes were subsequently cloned into the pComb3X vector as described before [38,39]. Briefly, LC genes and pComb3X vector were double-digested with *SacI/XbaI* restriction enzymes (New England Biolabs, Catalog No. R3156S and R0145S), purified using Wizard SV Gel and PCR Clean-Up System kit (Promega, Catalog No. A9281), and ligated at 23°C for 20 h with 2 U of T4 DNA ligase (Thermo Fisher Scientific, Catalog No. EL0011). The murine LC library and Fd genes were double-digested with *SpeI/XhoI* restriction enzymes (New England Biolabs Inc, Catalog No. R3133S and R0146S) and ligated as described above.

Hybrid Fab library

The human LC naïve library and the selected murine Fab clone were double-digested with *SpeI/XhoI*. The

human LC naïve library and the murine Fd gene were purified from 1% agarose gel and ligated to generate the hybrid combinatorial Fab library.

Human Fab library

The human LC genes from the selected hybrid Fab clones were amplified by PCR containing 0.8 mM dNTPs, 1.25 U Platinum *Taq* DNA polymerase High Fidelity (Thermo Fisher Scientific, Catalog No. 11304011), 1.5 mM MgCl₂, PCR Buffer 1× (Thermo Fisher Scientific, Catalog No. 11304011), 0.4 μM primer forward (5' GAGGAGGAG GAGGAGGAGGCGGGGCCAGGCGGCCGAG-CTC 3') and reverse (5' GGCCATGGCTGGTT GGCAGC 3') and 100 ng Fab clone. The PCR conditions were: 2 min at 94°C followed by 40 cycles of a three-step program (94°C, 1 min; 56°C, 1 min; 72°C, 1 min). After the final extension at 72°C for 5 min, the PCR products were analyzed through 1% agarose gel. The PCR-amplified human LC genes and the human Fd naïve library were double-digested with *SacI/XbaI*, purified, and ligated to generate the human combinatorial Fab library.

Phage display and panning of the combinatorial Fab libraries

The constructed combinatorial Fab libraries were electroporated into *Escherichia coli* XL1-Blue cells (Agilent Technologies, Catalog No. 200249), and the size of the libraries was measured. The bacteria infection with the helper phage VCSM13 (Agilent Technologies, Catalog No. 200251) and the phage display were performed as described before [39]. Five (or four) consecutive panning rounds were performed to enrich phages-displaying Fab that reacts with rFGF2 antigen. The plasmid constructed to express FGF2 was kindly provided by Dr. Maria Leonor Sarno de Oliveira (Butantan Institute, Brazil), and rFGF2 was produced as previously described [40]. The rFGF2 was coated on 96 well half-area microplates (Sigma-Aldrich, Catalog No. CLS3690) at 5 μg/mL. The wells were blocked with 3% BSA in TBS, washed with TBS, and the phages-displaying Fab library was added to the wells. For the human Fab library, the phages-displaying Fab were previously incubated with blocking solution (1% skim milk and 1% BSA) before being added to the rFGF2 coated

wells. After washing to remove unbound phages, the bound phages were eluted with 0.1 M HCl – glycine pH 2.2, then neutralized with 2 M Tris solution and amplified through *E. coli* XL1-Blue cells infection for the subsequent panning round. The phages-displaying Fab samples before the binding to the rFGF2 were called input phages, and the phages-displaying Fab recovered after binding to rFGF2 were determined as output phages. These samples were used to infect *E. coli* XL1-Blue cells, and the resulting CFU was counted to measure the panning efficiency. We established the bound percentage as the relation between output and input phages multiplied by 100. The enrichment rate was calculated as the ratio of the bound percentage from one panning round compared to the previous one.

Phage ELISA for screening combinatorial Fab libraries

Polyclonal phage ELISA analyzed the phage pools eluted from each panning round by binding to the antigen of interest rFGF2 and an irrelevant antigen (BSA). rFGF2 (or BSA) at 5 μg/mL was coated on 96 well half-area microplates, the wells were washed with PBS, blocked with 5% skim milk diluted in PBS, and incubated with about 10 [11] PFU of amplified phage pools. After washing, the HRP-conjugated mouse anti-M13 (Cytiva, Catalog No. 27-9421-01) was added to the wells, followed by another washing step. Next, the chromogenic solution of TMB (3,3',5,5' – tetramethylbenzidine) (Sigma-Aldrich, Catalog No. T0440) with H₂O₂ was added, and the reaction was stopped with 4.7 N of H₂SO₄. The absorbance was measured at 450 nm (Abs 450 nm). Monoclonal phage ELISA was performed to identify anti-FGF2 Fab individual clones. For the murine Fab library, after five panning rounds, single colonies carrying the phagemid from the fourth and fifth panning rounds were picked up and grown in 5 mL of SB medium with 100 μg/mL ampicillin, 10 μg/mL tetracycline and 40 mM glucose at 37°C for 7 h, 200 rpm. Phage amplification by infection with helper phage VCSM13 was performed as previously described [38], and the ELISA, as described above, was made to screen the phages-displaying Fab.

For the hybrid and human Fab libraries, 96-well polypropylene plates (Greiner Bio-One, Catalog

No. 650261) containing 200 μ L/well of SB medium with 100 μ g/mL ampicillin and 40 mM glucose were inoculated with single colonies carrying the phagemid from the last panning round and incubated at 37°C for 18 h, 220 rpm (pre-inoculum). Twenty microliters of each pre-inoculum were transferred to wells of a new plate containing 180 μ L of SB medium with 100 μ g/mL ampicillin, 40 mM glucose, and 10 [9] PFU of helper phage VCSM13 and were cultured at 37°C for 4 h, 220 rpm. The plate was centrifuged (2000 \times g; 4°C; 40 min), and the supernatant was removed. The cell pellet was resuspended in 200 μ L of SB, medium with 100 μ g/mL ampicillin and 70 μ g/mL kanamycin, and incubated at 30°C for 18 h, 220 rpm. After another centrifugation, the supernatant containing the phages-displaying Fab was used for screening by ELISA. The clone's selection was based on the ratio between the absorbance of rFGF2 over the absorbance of BSA binding. The clones resulting in a ratio greater than 8 [41] and absorbance to rFGF2 greater than 0.3 were defined as clones with higher binding to FGF2.

LC and Fd sequence analysis

The *E. coli* XL1-Blue was infected with the phage-displaying Fab clones with higher binding to rFGF2 and cultured in SB medium with 100 μ g/mL ampicillin for the phagemid extraction and analysis of the LC and Fd inserts through 1% agarose gel after double-digestion with *SacI/XbaI* and *SpeI/XhoI* restriction enzymes, respectively. The clones with LC and Fd genes were submitted to DNA sequencing by the Sanger method using ompseq (5' AAGACAGCTATCGCGATTGCAG 3') and pelseq (5' CTATTGCCTACGGCAGCCGCTG 3') primers for the LC and Fd genes amplification. Nucleotide sequences were translated into amino acids using the ExPASy Translate tool (web.expasy.org/translate/) and aligned using the EMBL-EBI Clustal Omega multiple sequence alignment (www.ebi.ac.uk/Tools/msa/clustalo/). CDR sequences were defined using VBASE2 (www.vbase2.org/).

Soluble Fab expression and characterization

Clones with different amino acid sequences were expressed as soluble Fab in *E. coli* TOP10F'

(Thermo Fisher Scientific, Catalog No. C303003). Two irrelevant Fab were used as negative controls: the murine anti-digoxin Fab [39] and the human anti-tetanus toxin Fab (anti-TT; pComb3XTT) [42]. After transforming the phagemid vector in *E. coli* TOP10F' [43], the bacteria were grown in 20 mL of SB medium with 100 μ g/mL ampicillin and 20 mM MgCl₂ until the log phase (Abs 600 nm = 0.6). The soluble Fab expression was induced with 0.5 mM IPTG at 25°C for 20 h, 200 rpm. Bacteria were harvested by centrifugation (8,000 \times g; 4°C; 30 min), and the bacteria pellet was suspended in 1 mL PBS, sonicated (10 cycles with 10 s pulse, 2 min interval in ice bath between each cycle) with amplitude 4 in the Ultrasonic Cell Disruptor Microson sonicator (Misonix) and centrifuged again (20,000 \times g; 4°C; 30 min) to obtain the lysate supernatant. Soluble Fab concentration was determined by sandwich ELISA as previously described [39]. Western blot was performed to assess the presence of Fab in the lysate supernatant samples. Lysates were subjected to SDS-PAGE 12% and transferred to PVDF membranes (Cytiva, Catalog No. 10600021), previously treated with methanol. The membranes were blocked with 10% skim milk in PBS and incubated with the HRP-conjugated AffiniPure F(ab')₂ Fragment Goat Anti-Mouse IgG, F(ab')₂ fragment specific (Jackson ImmunoResearch Laboratories, Catalog No. 115-036-072) or the HRP-conjugated Goat Anti-Human IgG(H+L) (Southern Biotech, Catalog No. 0109-05). Detection was performed using the chemiluminescence Amersham ECL Prime Western Blotting Detection Reagent kit (Cytiva, Catalog No. RPN2232) with exposure to photographic Hyperfilm™ ECL™ film (Cytiva, Catalog No. 28906835). The binding of Fab to the antigen of interest was analyzed by ELISA in microplates coated with 5 μ g/mL of rFGF2 (or BSA). Blocking was performed with 1% BSA in PBS, and the lysate supernatant, containing the soluble Fab from the clones, was added to the wells. After washing, the HRP-conjugated AffiniPure F(ab')₂ Fragment Goat Anti-Mouse IgG, F(ab')₂ fragment specific or the HRP-conjugated Goat Anti-Human IgG(H+L) was added as the secondary antibody. ELISA was developed as described above.

Generation of human anti-FGF2 mAbs

The human variable chains genes selected during the humanization process by guided selection were amplified using specific primers, according to the V and J classification, and cloned into the AbVec2.0-IGHG1, AbVec1.1-IGKC or AbVec1.1-IGLC2-XhoI vectors (kindly provided by Dr. Hedda Wardemann, German Cancer Research Center, Germany), which contains the constant region of the human immunoglobulin chains, as previously described [44]. The VH and VL genes of the selected murine Fab clone were cloned into the AbVec2.0-IGHG1 and AbVec1.1-IGKC vectors, respectively, to generate the chimeric anti-FGF2 antibody. A pair of the constructed LC and HC vectors were used for transient co-transfection of FreeStyle™ 293-F HEK cells to express the human (and chimeric) anti-FGF2 mAbs [44]. The mAbs were purified by affinity chromatography using protein-A sepharose (Cytiva, Catalog No. 17096303) in the Äkta Purifier System (Cytiva). The mAb concentration was determined by absorbance at 280 nm using the NanoDrop™ One/One^C Microvolume UV-Vis Spectrophotometer (Thermo Fisher Scientific).

Binding assay of human anti-FGF2 mAbs to rFGF2 by SPR

The binding ability of the human (and chimeric) anti-FGF2 mAbs to the rFGF2 was assessed by SPR in the BIAcore T200® system (Cytiva). All assays were carried out at 25°C in PBS-EP running buffer (PBS pH 7.4, with 3 mM EDTA and 0.005% Tween 20). BiaEvaluation Software (v3.0) was used to analyze the sensorgrams. An irrelevant human mAb (IgG negative ctrl) was included in all assays. The rFGF2 was immobilized on a CM5 sensor chip by amine coupling according to the manufacturer's instructions. Antibody samples diluted to 25 µg/mL were injected (60 s association and 30 s dissociation, 20 µL/min), and the sensor surface was regenerated between each sample (15 µL, 2 M NaCl). The binding resonance values (resonance units – RU) were recorded 10 s after the end of the sample injection (stability report point). The binding kinetics of

either human or chimeric anti-FGF2 mAbs to rFGF2 were evaluated using the multiple-cycle approach. Five concentrations of each anti-FGF2 mAb sample, starting at 25 µg/mL (3-fold dilution), were injected into the immobilized rFGF2 for 180 s at 30 µL/min. After dissociation (600 s), the sensor chip surface was regenerated (15 µL, 2 M NaCl). The association (k_a) and dissociation (k_d) constants were calculated by the Langmuir 1:1 interaction model.

Trypan blue proliferation assay

HUVEC and SK-Mel-28 cells (2×10^3 cells/100 µL/well) were plated on 96-well plates (Sigma-Aldrich, Catalog No. CLS3361) and cultured for 24 h with 5% CO₂ at 37°C. The wells were washed with PBS, and the cells were incubated with fresh culture medium containing 20 µg/mL of the anti-FGF2 mAbs, irrelevant human mAb (IgG negative ctrl), or PBS. After 72 h, cells were harvested and counted using a hemocytometer. The number of viable cells was determined by the trypan blue dye exclusion test. The experiment was performed in quadruplicate.

In vitro scratch assay

HUVEC and SK-Mel-28 cells (0.75×10^5 cells/500 µL/well) were cultured on 24-well plates (Sigma-Aldrich, Catalog No. CLS3524) with 5% CO₂ at 37°C until confluence. Each confluent monolayer was scratched using a 200 µL pipette tip to create a cell-free area. Cells were washed twice with PBS and incubated with fresh culture medium containing 20 µg/mL of the anti-FGF2 mAbs, irrelevant human mAb (IgG negative ctrl), or PBS, and incubated at 37°C, with 5% CO₂, for 48 h. The scratch area was photographed at 0 h and 48 h using Nikon Eclipse TE 300 inverted microscope coupled to a Nikon Digital Sight DS-Ri1 camera. The cell-free area was calculated using the ImageJ software (<https://imagej.nih.gov/ij/>). Cell migration analysis was performed by calculating the percentage of the regenerated area after 48 h of the experiment. The experiment was performed in duplicates.

Epitope prediction by molecular docking

Intermolecular interaction between the human (and chimeric) anti-FGF2 mAbs and FGF2 (PDB ID: 1bfg) was analyzed by molecular docking assay. Three-dimensional structural models of the antibody Fv region were produced using AbodyBuilder web server [45] with Sphinx [46] *ab initio* modeling algorithm to predict CDR H3 conformation. The docking of the antibody-antigen complexes was performed with HADDOCK web server [47] following the protocol described before [48]. The quality of output complex models and the performance of the docking method were assessed by the Critical Assessment of Predicted Interactions (CAPRI) criteria [49] based on the interface root-mean-square deviation (I_RMSD), ligand root-mean-square deviation (L_RMSD), and the fraction of native contacts reproduced in the predicted docking model (F_{nat}). Complex models with higher quality were visualized using PYMOL (v2.1), and the residues involved in the antibody-antigen interaction were determined with LigPlot⁺ (v2.2.4), using DIMPLOT program [50].

Statistical analysis

Statistical differences between groups were evaluated with GraphPad PRISM software (v.7) using one-way ANOVA followed by Bonferroni's posttest. $P < 0.05$ was considered significant.

Results

Selection of a murine Fab clone with higher binding to the rFGF2 from the combinatorial murine Fab library

The cDNA obtained from 3F12E7 hybridoma cells secreting murine anti-FGF2 mAb was used to amplify LC and Fd genes by PCR. For the construction of the murine Fab library, murine LC and Fd genes were cloned sequentially into the pComb3X vector, resulting in a library size of 2.4×10^7 [5] clones. The phages-displaying murine Fab were selected against rFGF2 through consecutive panning rounds. The total phage number before (input) and after (output) the panning procedure and the bound percentage are shown for

each panning round (Figure 1a). Although the bound percentage and the enrichment rate decreased in the first three rounds, probably due to an increase in the number of washes after the phage's incubation with the rFGF2, it increased in the fourth round. Polyclonal phage ELISA confirmed the enrichment of the murine Fab library against rFGF2 over five panning rounds (Figure 1b). Out of 54 single clones, 20 showed higher binding to rFGF2 when tested in monoclonal phage ELISA (Table 1; Supplementary Figure S1), by the criteria stated in the Material and Methods session. All 20 clones had the Fd gene, and 17 presented the LC gene (Table 1; Supplementary Figure S2). Deduced amino acid sequence from DNA sequencing showed six clones (11, 15, 17, 20, 22, and 23) with different sequences in framework 1 of Fd and LC genes (data not shown). The expression of the six murine Fab clones was confirmed by WB, revealing a band of about 50 kDa (Figure 2a). An additional band of 25 kDa, corresponding to the single LC or Fd proteins, was also observed (Figure 2a). All murine Fab clones were specific for the rFGF2 in ELISA (Figure 2b) without binding to the irrelevant antigen (BSA) (Supplementary Figure S3). Murine Fab clone 15 showed higher binding to the rFGF2 and was selected as a template for its humanization by guided selection.

Selection of three hybrid Fab clones with higher binding to the rFGF2 from the combinatorial hybrid Fab library

The hybrid Fab library was constructed by cloning the murine Fd gene (clone 15) into the human LC gene repertoire library and presented 4.4×10^7 [7] clones. Four panning rounds were performed to enrich the hybrid Fab library with clones binding to the rFGF2. A 6-fold increase in the bound percentage was observed in the second panning round compared to the previous one, and it remained almost constant in the following rounds (Figure 1c). Polyclonal phage ELISA demonstrated an increase in phages-displaying hybrid Fab against rFGF2 in the second, third, and fourth panning rounds, showing the hybrid Fab library enrichment with the target antigen (Figure 1d). A total of 180 single clones from the third and fourth panning

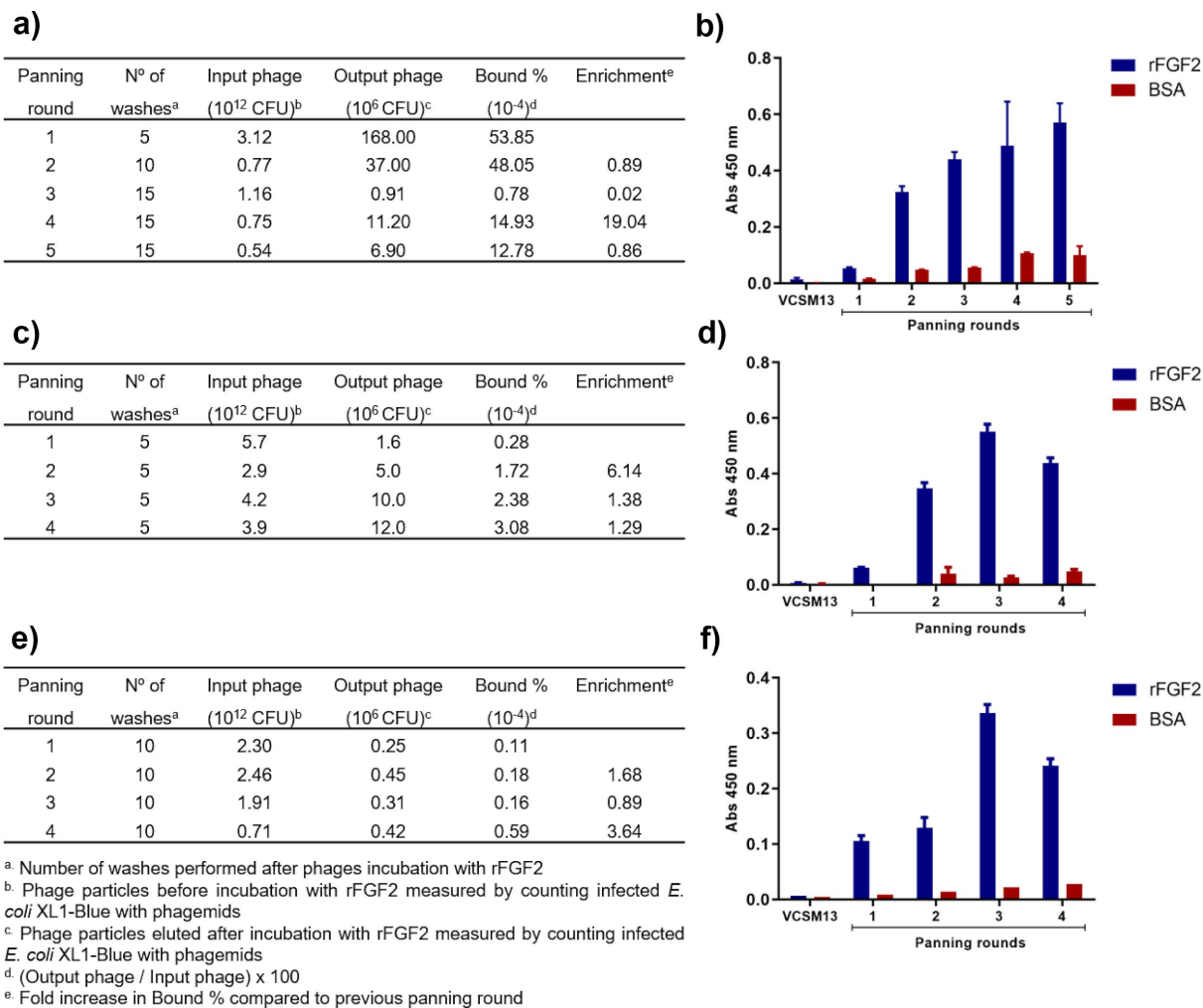


Figure 1. Characterizing the phages obtained from each panning round after amplifying the murine, hybrid and human Fab phage library. Phage particles before (input) and after (output) each panning round, bound percentage to rFGF2, and library enrichment for the murine (a), hybrid (c), and human (e) Fab phage library. The phage binding profiles from each panning round were obtained from the murine (b), hybrid (d), and human (f) Fab phage library by polyclonal phage ELISA. Helper phage VCSM13 was added as a negative control.

Table 1. Verification of the LC and Fd genes in clones with higher binding to rFGF2 selected from the three Fab libraries by monoclonal phage ELISA.

Library	Monoclonal phage ELISA ^a	Clones with LC gene ^b	Clones with Fd gene ^b	Complete clones (LC and Fd genes) ^b
Murine	20/54	17/20	20/20	17/20
Hybrid	24/180	18/24	24/24	18/24
Human	19/360	12/19	19/19	12/19

^aNumber of the clones with higher binding to rFGF2/number of total clones tested.

^bNumber of the clones with antibody gene/number of the total clones tested.

rounds were selected, resulting in variable binding to rFGF2 in monoclonal phage ELISA (Supplementary Figure S4), and 24 clones were selected as higher binders to rFGF2 (Table 1). Of these clones, all presented the Fd gene, and 18 the LC gene (Table 1; Supplementary Figure 5). Deduced amino acid sequences from the Fd gene of the 18 complete

clones showed murine sequence, and six clones (7, 10, 32, 40, 62, and 85) presented different LC sequences; the rest of them exhibited stop codon in the LC sequence (data not shown).

Those six hybrid Fab clones were expressed and confirmed by WB showing a band of about 50 kDa immunodetected with both the HRP-conjugated

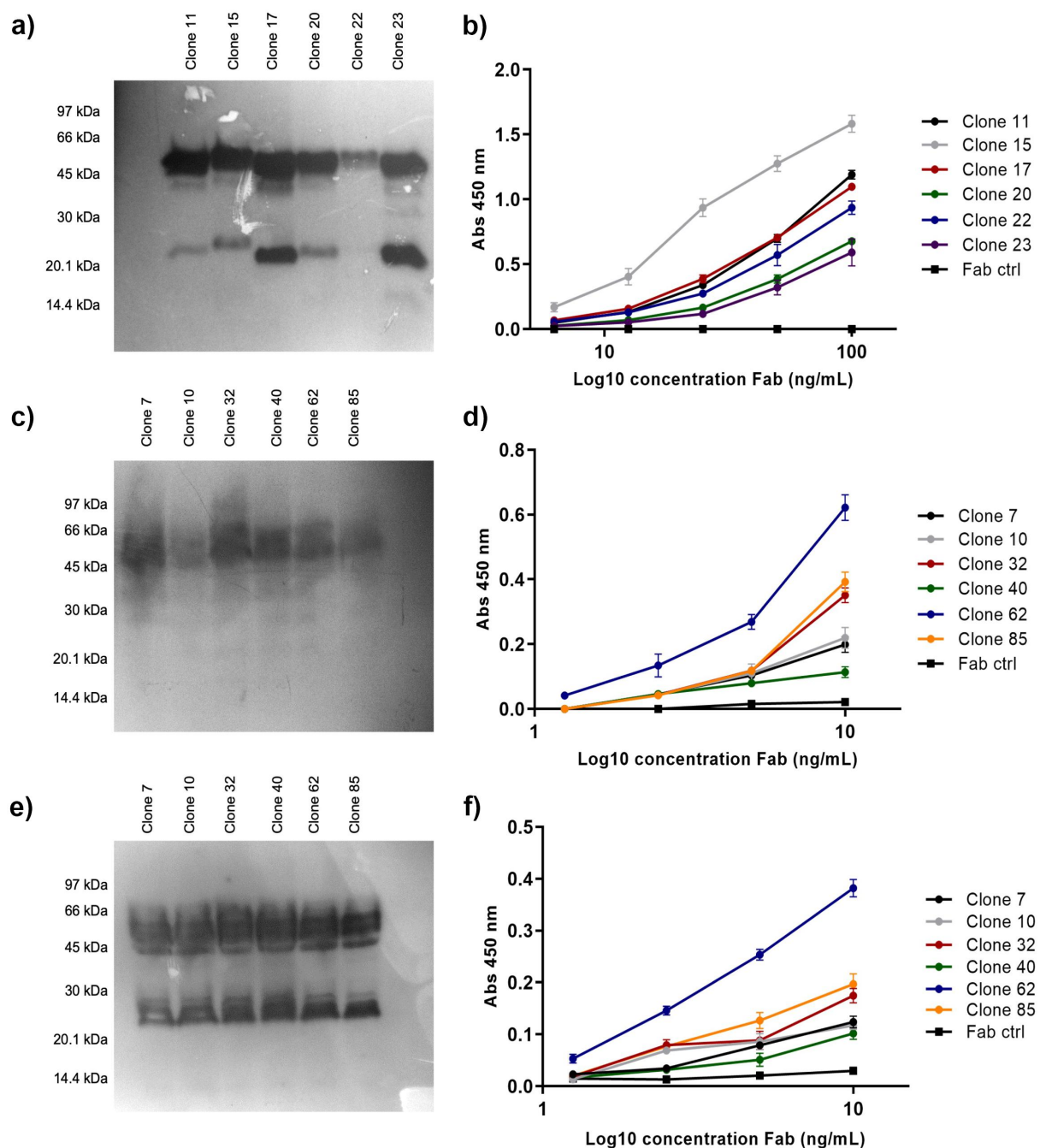


Figure 2. Binding analysis to rFGF2 of murine and hybrid Fab expressed in *E. coli* TOP10F.

WB analysis of murine (a) and hybrid Fab clones' immunodetected with the HRP-conjugated AffiniPure F(ab')₂ Fragment Goat Anti-Mouse IgG, F(ab')₂ fragment specific (c) and the HRP-conjugated Goat Anti-Human IgG(H+L) (e). Binding of the murine Fab clones (b) and the hybrid Fab clones to rFGF2 by ELISA using the HRP-conjugated AffiniPure F(ab')₂ Fragment Goat Anti-Mouse IgG, F(ab')₂ fragment specific (d) and the HRP-conjugated Goat Anti-Human IgG(H+L) (f) as the secondary antibody. Soluble Fabs in the lysate supernatant were added in rFGF2 (or BSA) coated wells. BSA (negative control) absorbance values range from 0.002 to 0.029. Results show the mean absorbance of duplicates and the standard deviation.

AffiniPure F(ab')₂ Fragment Goat Anti-Mouse IgG, F(ab')₂ fragment specific (Figure 2c) and the HRP-conjugated Goat Anti-Human IgG(H+L) (Figure 2e). In addition, a band of about 25 kDa

was observed in the samples immunodetected with HRP-conjugated Goat Anti-Human IgG(H+L), indicating the presence of human LC protein (Figure 2e). The soluble hybrid Fab clones showed

different binding profiles to the rFGF2 (Figure 1d) and no binding to the irrelevant antigen (BSA) (Supplementary Figure S6). The hybrid Fab clones 32, 62, and 85 showed higher binding to the rFGF2 and were selected for the next step of the humanization process by guided selection.

Selection of eight human Fd sequences against rFGF2 from the combinatorial human Fab library

The human LC genes of the hybrid Fab clones (32, 62, and 85) were cloned into the vector containing the human Fd gene repertoire library to construct the human Fab library. As a result, a library with an estimated size of 2.4×10^8 [8] clones was obtained. We performed four panning rounds to enrich phages-displaying human Fab with high binding to rFGF2. The bound percentage of Fabs was higher in the fourth panning round compared to the precedent (Figure 1e). The polyclonal phage ELISA showed that the library was enriched with phages-displaying human Fab against rFGF2 through the four panning rounds. A higher binding rate was attained in the third round (Figure 1f). From 360 individual clones analyzed by the monoclonal phage ELISA, 19 were higher binders to rFGF2 (Table 1; Supplementary Figure S7). All 19 clones presented the Fd gene, and 12 presented the LC gene (Table 1; Supplementary Figure S8). The DNA sequencing of the 12 clones presenting both antibody genes was performed (data not shown), and the deduced amino acid sequences showed stop codons in the LC sequence of all the clones, producing nonfunctional chains and making not possible the selection of complete human Fab clones. Out of 12, eight clones (24, 29, 88, 89, 98, 109, 117, and 119)

presented different Fd sequences and were used to generate the human anti-FGF2 mAbs.

Expression of 20 human (and one chimeric) anti-FGF2 mAbs

To circumvent the fact that it was not possible to select the complete human Fab by the guided selection, we cloned the three human LC sequences and the eight human Fd sequences selected through the phage display humanization process into AbVec vectors [44], containing the constant region of the human IgG1 or the kappa or lambda LC. The VH and VL genes of murine Fab clone 15 were cloned into the AbVec vectors to generate the chimeric anti-FGF2 mAb, used as a positive control in the binding and in vitro functional assays. The eight AbVec HC clones were combined with the three LC clones for co-transfection of FreeStyle™ 293-F HEK cells. The IgG expression succeeded in 20 out of 24 possible combinations. The supernatants containing mAbs of the 20 combinations plus the chimeric anti-FGF2 were purified through protein A affinity chromatography and quantified for the assays.

Seven human mAbs showed binding to rFGF2 by SPR

The 20 human anti-FGF2 mAbs binding to the rFGF2 was evaluated by SPR with rFGF2 immobilized in the sensor. The resulting RU values were determined from the sensorgrams obtained at the binding stability point. Some mAbs showed minimal binding to the rFGF2, a result close to that obtained by irrelevant human mAb (IgG negative ctrl), and were excluded. Seven

Table 2. Human (and chimeric) anti-FGF2 mAbs binding, k_a , k_d e K_D values determined by SPR assays.

Antibody	RU	k_a ($M^{-1} \cdot s^{-1}$)	k_d (s^{-1})	K_D (M)
Chimeric	1683.00	$(1.67 \pm 0.37) \times 10^5$	$(9.58 \pm 2.29) \times 10^{-5}$	$(6.03 \pm 2.69) \times 10^{-10}$
32L98H	228.50	$(2.49 \pm 1.88) \times 10^5$	$(3.74 \pm 0.68) \times 10^{-3}$	$(2.23 \pm 1.95) \times 10^{-8}$
62K88H	223.60	$(0.98 \pm 0.81) \times 10^5$	$(0.96 \pm 0.99) \times 10^{-3}$	$(0.86 \pm 0.30) \times 10^{-8}$
32L109H	210.00	$(1.33 \pm 0.74) \times 10^5$	$(2.80 \pm 1.47) \times 10^{-3}$	$(2.87 \pm 2.71) \times 10^{-8}$
62K98H	204.00	$(1.20 \pm 0.72) \times 10^5$	$(1.21 \pm 0.49) \times 10^{-3}$	$(1.08 \pm 0.24) \times 10^{-8}$
32L88H	86.07	$(1.72 \pm 0.64) \times 10^5$	$(1.80 \pm 0.99) \times 10^{-3}$	$(1.24 \pm 1.03) \times 10^{-8}$
85L117H	25.91	$(0.71 \pm 0.31) \times 10^5$	$(0.96 \pm 0.17) \times 10^{-3}$	$(1.43 \pm 0.38) \times 10^{-8}$
62K29H	22.25	$(2.35 \pm 2.49) \times 10^5$	$(1.14 \pm 1.34) \times 10^{-2}$	$(4.20 \pm 1.26) \times 10^{-8}$
IgG negative ctrl	5.69	-	-	-

(mean \pm SD, $n = 2$).

human mAbs bound to rFGF2 immobilized in the sensor with resonance values above 20 RU and were further analyzed by kinetic affinity assays (Table 2 and Supplementary Figure S9). The human anti-FGF2 mAbs showed k_a values close to those obtained by the chimeric anti-FGF2, although higher k_d values indicated faster dissociation and resulted in lower kinetic affinity (higher K_D values) (Table 2).

Two human anti-FGF2 mAbs were able to attenuate HUVEC and SK-Mel-28 cell proliferation and migration

The functional activity of the human anti-FGF2 mAbs was assessed by in vitro assays with HUVEC and SK-Mel-28 cells. The human anti-FGF2 62K98H

and 85L117H mAbs (as well as the chimeric anti-FGF2 mAb) significantly reduced the number of HUVEC (Figure 3a) and SK-Mel-28 (Figure 3d) viable cells compared to the irrelevant human mAb (IgG negative ctrl) in the proliferation assay with trypan blue exclusion. In the same trend, HUVEC and SK-Mel-28 cells incubated with the human anti-FGF2 62K98H and 85L117H mAbs (as well as the chimeric anti-FGF2 mAb) showed attenuated cell migration in a monolayer scratch assay. First, the kinetics migration index was assayed with the chimeric mAb in HUVEC cells at 16, 20, 24, and 48 h showing statistical significance from the PBS and isotype controls at all time points. SK-MEL-28 cells were assayed for 24 and 48 h for all the samples, and the statistical significance increased at a longer time (data not shown). The results taken at 48 h are

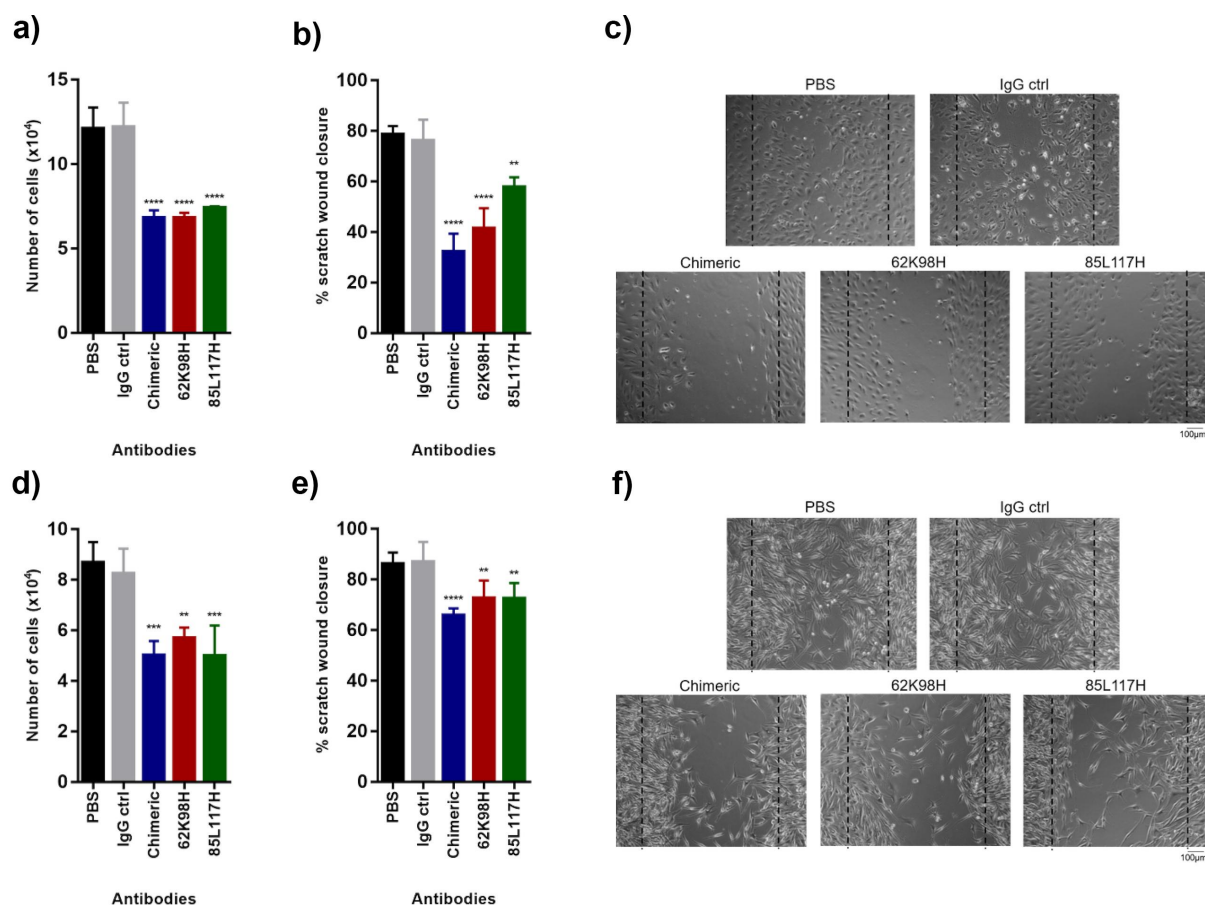


Figure 3. In vitro functional activity of the human (and chimeric) anti-FGF2 mAbs.

The human anti-FGF2 62K98H and 85L117H mAbs reduced in vitro HUVEC (a) and SK-Mel-28 (d) proliferation and attenuated HUVEC (b) and SK-Mel-28 (e) cell migration. Cells were incubated with 20 $\mu\text{g}/\text{mL}$ of the indicated mAbs. Cell proliferation and migration were assessed by trypan blue proliferation and scratch assays, respectively. Representative micrographs of the scratch assay on HUVEC (c) and SK-Mel-28 cells (f). The dashed lines indicate the original cell-free area. Scale bar, 100 μm . ** $p \leq 0.01$; *** $p \leq 0.001$; **** $p \leq 0.0001$ compared to irrelevant human mAb (IgG negative ctrl); one-way ANOVA/Bonferroni's posttest.

presented in Figure 3 (3B, 3E, 3C, and 3F). Such results are comparable to those previously demonstrated with the murine anti-FGF2 3F12E7 mAb [25] used as template in the humanization process.

Molecular docking assay predicted a similar epitope recognition by the two human anti-FGF2 and the chimeric anti-FGF2 mAbs

In silico molecular docking predicted the binding interface residues between the best structural model of antibody Fv region generated by ABodyBuilder and the FGF2 (PDB ID: 1bfg). Following the CAPRI criteria for high-quality models ($F_{\text{nat}} \geq 0.5$ and I-RMSD ≤ 1.0 or L-RMSD ≤ 1.0) [49], 11 complex models were selected for the chimeric anti-FGF2 mAb, six for the human anti-FGF2 62K98H mAb, and four for the human anti-FGF2 85L117H mAb (Table 3). In addition, the output complex model that presented a lower I-RMSD value from each antibody was chosen to analyze the critical residues involved in antigen binding using the LigPlot⁺/DIMPLLOT.

The chimeric anti-FGF2 mAb was predicted to contact the FGF2 residues Tyr111 and Tyr124 (Figure 4a) within the FGFR and heparin-binding domains in FGF2 [51,52] while the human anti-FGF2 62K98H and 85L117H mAbs were predicted to contact the FGF2 residues R120, Y124 (Figure 4b), and K119, Q123, Y124 (Figure 4c),

respectively, within the heparin-binding domains in FGF2 [52]. The inhibition of such FGF2 function-related domains by the human and chimeric anti-FGF2 mAbs might interfere with the FGF2 function via signal transduction, which was observed by impaired cell proliferation and migration (Figure 3). The human anti-FGF2 62K98H and 85L117H mAbs were predicted to contact the FGF2 at a similar patch of residues than the chimeric anti-FGF2 mAb (Figure 4d). This result might show that the human anti-FGF2 mAbs recognized the same epitope as the chimeric anti-FGF2, suggesting the success of the humanization method in generating human antibodies corresponding to the murine anti-FGF2 3F12E7 mAb.

Discussion

Anti-FGF2 antibodies have been proposed by different research groups as of murine mAbs produced by hybridoma technology and evaluated through in vivo models of hepatocellular carcinoma, Lewis lung carcinoma, and melanoma [25,53–55]. Also, a humanized antibody by CDR grafting was tested in an experimental model of non-small cell lung cancer [56]. A human antibody could inhibit the in vitro proliferation of glioblastoma cells [57]. In addition, these antibodies were accomplished to impair tumor cell proliferation, angiogenesis,

Table 3. Top output complex models selected based on CAPRI criteria.

Antibody	I-RMSD	L-RMSD	F_{nat}
Chimeric complex 49	0.401	4.180	0.694
Chimeric complex 95	0.478	3.564	0.764
Chimeric complex 122	0.407	0.914	0.847
Chimeric complex 144	0.470	1.728	0.861
Chimeric complex 200	0.760	2.153	0.792
Chimeric complex 217	0.296	0.461	0.875
Chimeric complex 226	0.259	0.839	0.889
Chimeric complex 237	0.467	3.009	0.778
Chimeric complex 238	0.339	0.875	0.903
Chimeric complex 306	0.507	7.676	0.639
Chimeric complex 338	0.448	7.499	0.556
62K98H complex 5	0.335	2.564	0.758
62K98H complex 9	0.558	1.198	0.780
962K98H complex 15	0.158	2.601	0.736
62K98H complex 19	0.459	1.228	0.725
62K98H complex 21	0.303	1.646	0.769
62K98H complex 22	0.615	2.156	0.802
85L117H complex 154	0.755	4.106	0.506
85L117H complex 303	0.663	2.248	0.714
85L117H complex 311	0.558	3.412	0.558
85L117H complex 371	0.678	3.106	0.636

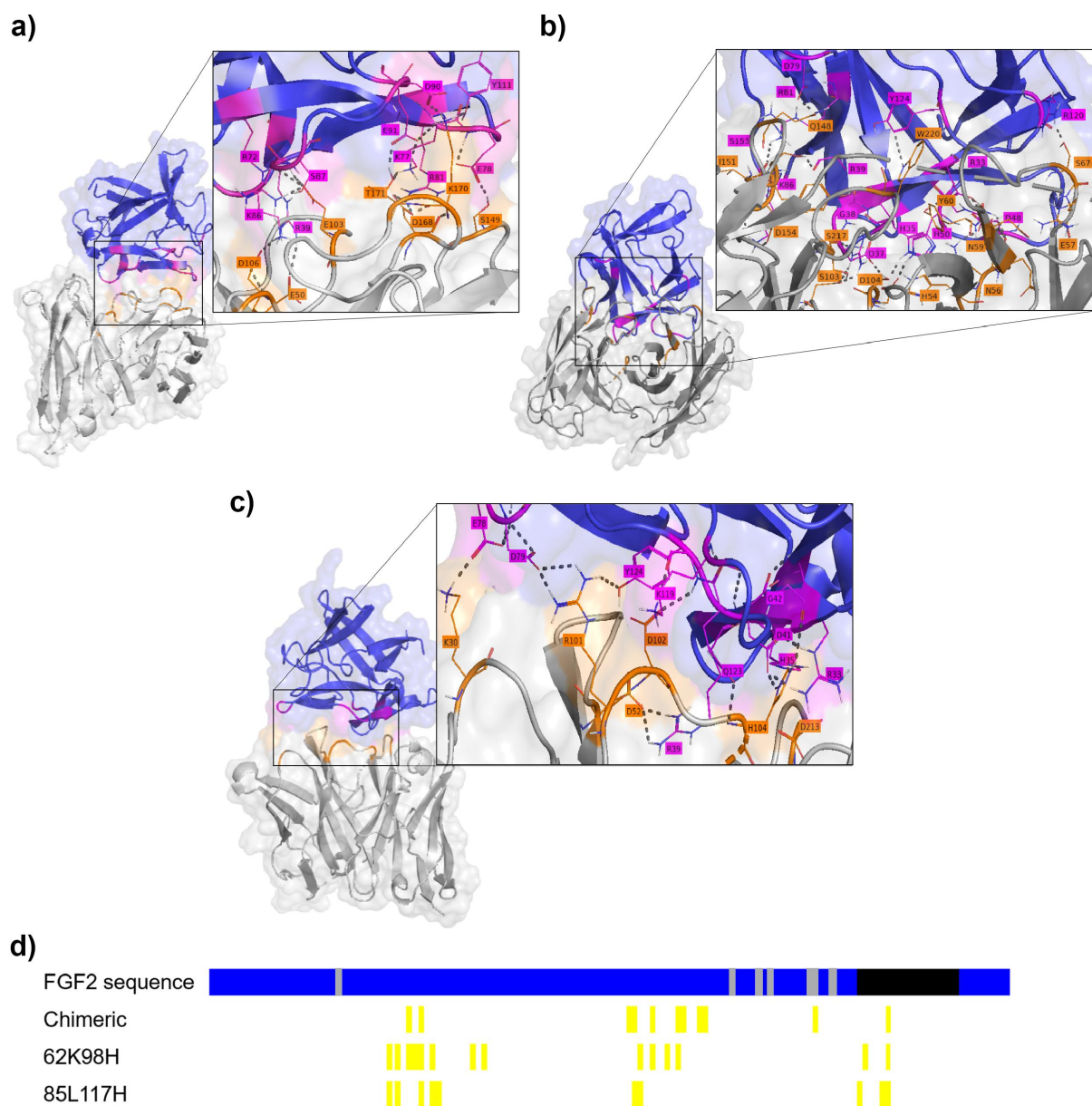


Figure 4. Prediction of human (and chimeric) anti-FGF2 62K98H and 85L117H antibodies binding to FGF2.

Three-dimensional representation of the chimeric (a), 62K98H (b), and 85L117H (c) antibody Fv region and FGF2 complexes. FGF2 and antibodies' residues found by LigPlot⁺/DIMPLLOT analyses are labeled magenta and orange, respectively. Dashed lines indicated the hydrogen bonds. d) Schematically representation in yellow of the FGF2 residues predicted to interact with the human (and chimeric) anti-FGF2 62K98H and 85L117H antibodies. The FGFR and heparin-binding sites are indicated in gray and black, respectively.

and/or metastasis [25,53–57]. Still, a mAb against FGF2 has not yet been approved for clinical use, and, to our knowledge, human anti-FGF2 mAbs have not yet been tested in an experimental melanoma model. The murine anti-FGF2 3F12E7 mAb presented promising results for use as an adjuvant in melanoma therapy when tested in mice [25]. However, murine antibodies can induce immunogenic

responses [3], decreasing therapeutic efficacy [58] and causing adverse effects [59].

Several antibody humanization techniques have been developed over recent years, with success in obtaining therapeutic antibodies [6]. The guided selection technique, used for the generation of the first human antibody approved by the FDA [19], allows the selection of fully human antibodies from combinatorial libraries, formed by the

human immunoglobulin gene and non-human antibody gene, by the enrichment with the antigen of interest [22]. This technique was chosen to humanize the murine anti-FGF2 3F12E7 mAb to obtain human antibodies similar to the murine version.

The guided selection procedure aimed to select Fab fragments; first, the murine Fab, followed by the hybrid Fab composed of a human LC with a murine Fd, and finally, a fully human Fab. Although a productive human anti-FGF2 Fab could not be reached, the human VL and VH genes selected through the panning steps by their binding to the target antigen rFGF2 were randomly assembled to generate full-length IgG. For that, the strategy consisted in cloning the individual VL and VH into vectors containing either the IgG1, kappa, or lambda constant region genes. By combining three VL and eight VH, 24 possibilities of different mAbs were possible by co-transfection of the cloned vectors. Twenty human anti-FGF2 mAbs were expressed, which entered the first challenge of binding to rFGF2 by SPR, resulting in the generation of seven human mAbs recognizing the target. The kinetic affinity of the human anti-FGF2 mAbs was 10^{-8} M, considered medium to high-affinity antibodies [60], despite being about 20 to 130 times lower than the chimeric anti-FGF2 mAb affinity. A decrease in affinity is often observed in antibody humanization processes [61–63] and may be due, in this case, to the human naïve library, composed mainly of IgM antibody genes. Although IgM antibodies have a lower affinity than IgG, naïve antibody libraries are more diverse. They may contain a repertoire of auto-reactive antibody genes [36,64], which is relevant when selecting antibodies against self-antigens, such as FGF2. The affinity of antibodies selected by phage display from libraries of naïve antibodies can be improved by carrying out other processes, such as affinity maturation, which is a feasible alternative to be explored for the human anti-FGF2 mAbs generated in this work, if needed. The anti-TNF- α Humira (adalimumab) is an example of a therapeutic antibody that underwent CDR mutagenesis after being humanized by the guided selection technique to produce the antibody with high affinity finally [19,24].

The seven human anti-FGF2 mAbs had their functional activity evaluated by in vitro cell proliferation and migration assays. Molecules capable of inhibiting these events are interesting for developing cancer therapies since, in endothelial cells, cell proliferation and migration are necessary for tumor dissemination, invasion, and angiogenesis [65–67]. Moreover, in tumor cells, these processes are key steps to trigger metastasis and cancer progression [68,69]. Two human anti-FGF2 mAbs – 62K98H and 85L117H – could reduce the number of viable cells in the cell proliferation assay and attenuate the migration of HUVEC and SK-Mel-28 cells. The decrease in proliferation and attenuation of cell migration was also observed in our study with the chimeric anti-FGF2 mAb and corroborated with the results obtained with the murine anti-FGF2 3F12E7 mAb [25,70].

The human anti-FGF2 62K98H and 85L117H mAbs, and the chimeric, had their epitope recognition predicted by in silico molecular docking assay. The antigen-antibody interaction showed that the human anti-FGF2 62K98H and 85L117H and the chimeric mAbs contact nearly the same region in the FGF2 surface, comprehending the heparin-binding domains. Since the interaction of FGF2 to its receptor, stabilized by heparin, is necessary for the FGF2-mediated signal transduction [28], it is possible to consider that the three anti-FGF2 mAbs (62K98H, 85L117H, and chimeric) reduced the HUVEC and SK-Mel-28 cell proliferation and migration by preventing the FGF2 binding to FGFR and then blocking the FGF2 signaling pathway. Furthermore, the human anti-FGF2 62K98H and 85L117H mAbs were predicted to contact the FGF2 at a similar patch of residues to the chimeric mAb. This result might show that the human anti-FGF2 mAbs recognized the same epitope as the chimeric anti-FGF2, suggesting the success of the humanization method in generating human mAbs corresponding to the murine anti-FGF2 3F12E7 mAb. The two human mAbs interact with FGF2 in the residues R120/Y124 and K119/Q123/Y124, within the binding domain of FGF2 to HSPG (heparan sulfate proteoglycans). This region is important for FGF2 functionality, once, to perform its function, FGF2 interacts with FGFR and with HSPG in

a ternary complex (FGF2-FGFR-HSPG), leading to signaling activation cascades related to proliferation, migration, and cellular differentiation [71]. The fact that humanization preserved the binding to the same epitope as the parental murine antibody previously characterized *in vitro* and *in vivo*, suggests potential for their use as adjuvant therapy for melanoma.

Altogether, the *in vitro* cell and *in silico* assays demonstrated the feasibility of the humanization approach used here to generate human anti-FGF2 mAbs with comparable properties to the murine parental mAb and expected to display similar control of melanoma progression. Besides the therapeutic use associated with melanoma and other tumors, such as angiogenesis inhibition, there are potential applications for anti-FGF2 mAbs in the control of fibrotic diseases, neutralizing the excessive action of FGF2, e.g. in diseases of intense tissue repair (keloids), and idiopathic fibrosis or secondary to chronic inflammatory diseases. In addition to the therapeutic expectation, the antibodies could be applied for immunoscintigraphy, labeled with radioisotopes, for molecular imaging and prediction of fibrosing responses.

Abbreviations

CDR: Complementarity-determining region; CFU: Colony forming unit; Ctrl: Control; Fab: Fragment antigen binding; FDA: U.S. Food and Drug Administration; FGF2: Fibroblast growth factor 2; Fv: Fragment variable; HC: Heavy chain; HUVEC: Human umbilical vein endothelial cell; IgG: Immunoglobulin G; LC: Light chain; mAb: Monoclonal antibody; PBMC: Peripheral blood mononuclear cells; PBS: Phosphate buffered saline; PFU: Plaque forming unit; SB: Super Broth; SK-Mel-28: Human melanoma cells; TBS: Tris-buffered saline; VH: Variable heavy domain; VL: Variable light domain

Acknowledgments

We thank Dr. Maria Leonor Sarno de Oliveira (Butantan Institute, Brazil) for providing the plasmid to express the FGF2. We are grateful to all the staff from the Laboratory of Biopharmaceuticals (Butantan Institute), specially

Roselaine Campos Targino and Camila Maria Lucia da Silva, for technical assistance.

Disclosure statement

CG Magalhães, LR Tsuruta, JZ de Moraes, and AM Moro are authors of a deposited patent.

Funding

This work was supported by FAPESP (2015/15611-0, 2020/07040-1) and Butantan Foundation. Fellowships were granted by CNPq (140274/2017-0 - CGM; 307045/2020-0- AMM).

Author contributions statement

CGM, CPM, TMM, WQ, AG, and JJM performed the experiments. JZM provided the hybridoma and contributed to the migration assay. AMM contributed with reagents, materials, and analysis tools. LRT provided human HC and LC libraries. LRT and AMM supervised the study and reviewed the manuscript. CGM, LRT, and AMM designed the experiments, analyzed and interpreted data, and wrote the manuscript. All authors approve the final version to be published and agree to be accountable for all aspects of the work.

Data availability statement

Data from this project is available at OSF <https://osf.io/ax8sn/files/osfstorage>

ORCID

Carolina Georg Magalhães  <http://orcid.org/0000-0001-7099-060X>

Jane Zveiter de Moraes  <http://orcid.org/0000-0003-2812-5887>

Lilian Rumi Tsuruta  <http://orcid.org/0000-0001-9647-7687>

Ana Maria Moro  <http://orcid.org/0000-0002-0650-7764>

References

- [1] Köhler G, Milstein C. Continuous cultures of fused cells secreting antibody of predefined specificity. *Nature*. 1975;256(5517):495–497. doi: 10.1038/256495a0
- [2] Emmons C, Hunsicker LG. Muromonab-CD3 (Orthoclone OKT3): the first monoclonal antibody approved for therapeutic use. *Iowa Med*. 1987;77(2):78–82.
- [3] Hwang WYK, Foote J. Immunogenicity of engineered antibodies. *Methods*. 2005;36(1):3–10. doi: 10.1016/j.ymeth.2005.01.001
- [4] Carter P. Improving the efficacy of antibody-based cancer therapies. *Nat Rev Cancer*. 2001;1(2):118–129. doi: 10.1038/35101072

- [5] Ober RJ, Radu CG, Ghetie V, et al. Differences in promiscuity for antibody–FcRn interactions across species: implications for therapeutic antibodies. *Int Immunol*. 2001;13(12):1551–1559. doi: [10.1093/intimm/13.12.1551](https://doi.org/10.1093/intimm/13.12.1551)
- [6] dos Santos ML, Quintilio W, Manieri TM, et al. Advances and challenges in therapeutic monoclonal antibodies drug development. *Braz J Pharm Sci*. 2018;54(spe):1–15. doi: [10.1590/s2175-97902018000001007](https://doi.org/10.1590/s2175-97902018000001007)
- [7] Antibody Society [Internet]. 2022 [cited 2022 Nov 24]; Available from: <https://www.antibodysociety.org/resources/approved-antibodies/>
- [8] Morrison SL, Johnson MJ, Herzenberg LA, et al. Chimeric human antibody molecules: Mouse antigen-binding domains with human constant region domains. *Immunology*. 1984;81(21):6851–6855. doi: [10.1073/pnas.81.21.6851](https://doi.org/10.1073/pnas.81.21.6851)
- [9] Güssow D, Seemann G. Humanization of monoclonal antibodies. *Methods Enzymol*. 1991;203:99–121.
- [10] Jones PT, Dear PH, Foote J, et al. Replacing the complementarity-determining regions in a human antibody with those from a mouse. *Nature*. 1986;321(6069):522–525. doi: [10.1038/321522a0](https://doi.org/10.1038/321522a0)
- [11] Verhoeyen M, Milsrein CE, Winter G. Reshaping human antibodies: Grafting an antilysozyme activity. *Sci* (1979). 1988;239(4847):1534–1536. doi: [10.1126/science.2451287](https://doi.org/10.1126/science.2451287)
- [12] Tempest PR, Bremner P, Lambert M, et al. Reshaping a human monoclonal antibody to inhibit human respiratory syncytial virus infection in vivo. *Nat Biotechnol*. 1991;9(3):266–271. doi: [10.1038/nbt0391-266](https://doi.org/10.1038/nbt0391-266)
- [13] dos Santos ML, Yeda FP, Tsuruta LR, et al. Rebma200, a humanized monoclonal antibody targeting the sodium phosphate transporter NaPi2b displays strong immune mediated cytotoxicity against cancer: A novel reagent for targeted antibody therapy of cancer. *PLoS One*. 2013;8(7):e70332. doi: [10.1371/journal.pone.0070332](https://doi.org/10.1371/journal.pone.0070332)
- [14] Tsuruta LR, dos Santos ML, Moro AM. Display technologies for the selection of monoclonal antibodies for clinical use. In: Böldicke T, editor. *Antibody engineering*. 2018. doi: [10.5772/intechopen.70930](https://doi.org/10.5772/intechopen.70930)
- [15] Barbas CF, Burton DR, Scott JK, et al. *Phage display: a laboratory manual*. New York: Cold Spring Harbor Laboratory Press; 2001.
- [16] Smith GP. Filamentous fusion phage: novel expression vectors that display cloned antigens on the virion surface. *Science*. 1985;228(4705):1315–1317. 1979. doi: [10.1126/science.4001944](https://doi.org/10.1126/science.4001944)
- [17] Frenzel A, Schirrmann T, Hust M. Phage display-derived human antibodies in clinical development and therapy. *MAbs*. 2016;8(7):1177–1194. doi: [10.1080/19420862.2016.1212149](https://doi.org/10.1080/19420862.2016.1212149)
- [18] Figini M, Obici L, Mezzanzanica D, et al. Panning phage antibody libraries on cells: Isolation of human Fab fragments against ovarian carcinoma using guided selection. *Cancer Res*. 1998;58(5):991–996.
- [19] Jespers LS, Roberts A, Mahler SM, et al. Guiding the selection of human antibodies from phage display repertoires to a single epitope of an antigen. *Bio/Technology*. 1994;12:899–903. doi: [10.1038/nbt0994-899](https://doi.org/10.1038/nbt0994-899)
- [20] Watzka H, Pfizenmaier K, Moosmayer D. Guided selection of antibody fragments specific for human interferon γ receptor 1 from a human VH- and VL-gene repertoire. *Immunotechnology*. 1998;3(4):279–291. doi: [10.1016/S1380-2933\(97\)10008-2](https://doi.org/10.1016/S1380-2933(97)10008-2)
- [21] Beiboer SHW, Reurs A, Roovers RC, et al. Guided selection of a pan carcinoma specific antibody reveals similar binding characteristics yet structural divergence between the original murine antibody and its human equivalent. *J Mol Biol*. 2000;296(3):833–849. doi: [10.1006/jmbi.2000.3512](https://doi.org/10.1006/jmbi.2000.3512)
- [22] Kim SJ, Hong HJ. Guided selection of human antibody light chains against TAG-72 using a phage display chain shuffling approach. *J Microbiol*. 2007;45:572–577.
- [23] Bao GQ, Li Y, Ma QJ, et al. Isolating human antibody against human hepatocellular carcinoma by guided-selection. *Cancer Biol Ther*. 2005;4(12):1374–1380. doi: [10.4161/cbt.4.12.2273](https://doi.org/10.4161/cbt.4.12.2273)
- [24] Osbourn J, Groves M, Vaughan T. From rodent reagents to human therapeutics using antibody guided selection. *Methods*. 2005;36(1):61–68. doi: [10.1016/j.ymeth.2005.01.006](https://doi.org/10.1016/j.ymeth.2005.01.006)
- [25] de Aguiar RB, Parise CB, Souza CRT, et al. Blocking FGF2 with a new specific monoclonal antibody impairs angiogenesis and experimental metastatic melanoma, suggesting a potential role in adjuvant settings. *Cancer Lett*. 2016;371(2):151–160. doi: [10.1016/j.canlet.2015.11.030](https://doi.org/10.1016/j.canlet.2015.11.030)
- [26] Shing Y, Folkman J, Sullivan R, et al. Heparin affinity: Purification of a tumor-derived capillary endothelial cell growth factor. *Science*. 1984;223:1296–1299. 1979. doi: [10.1126/science.6199844](https://doi.org/10.1126/science.6199844)
- [27] Moscatelli D, Presta M, Rifkin DB. Purification of a factor from human placenta that stimulates capillary endothelial cell protease production, DNA synthesis, and migration. *Proc Natl Acad Sci*. 1986;83(7):2091–2095. doi: [10.1073/pnas.83.7.2091](https://doi.org/10.1073/pnas.83.7.2091)
- [28] Akl MR, Nagpal P, Ayoub NM, et al. Molecular and clinical significance of fibroblast growth factor 2 (FGF2/bFGF) in malignancies of solid and hematological cancers for personalized therapies. *Oncotarget*. 2016;7(28):44735–44762. doi: [10.18632/oncotarget.8203](https://doi.org/10.18632/oncotarget.8203)
- [29] Gordon-Weeks AN, Lim SY, Yuzhalin AE, et al. Neutrophils promote hepatic metastasis growth through fibroblast growth factor 2–dependent angiogenesis in mice. *Hepatology*. 2017;65(6):1920–1935. doi: [10.1002/hep.29088](https://doi.org/10.1002/hep.29088)
- [30] Yu P, Wilhelm K, Dubrac A, et al. FGF-Dependent metabolic control of vascular development. *J Vasc Surg*. 2017;66(3):959. doi: [10.1016/j.jvs.2017.07.055](https://doi.org/10.1016/j.jvs.2017.07.055)
- [31] Korc M, Friesel RE. The role of fibroblast growth factors in tumor growth. *Curr Cancer Drug Targets*. 2009;9(5):639–651. doi: [10.2174/156800909789057006](https://doi.org/10.2174/156800909789057006)
- [32] Hu M, Hu Y, He J, et al. Prognostic value of basic fibroblast growth factor (bFGF) in lung cancer:

- A systematic review with meta-analysis. *PLoS One*. 2016;11(1):1–14. doi: [10.1371/journal.pone.0147374](https://doi.org/10.1371/journal.pone.0147374)
- [33] Ugurel S, Rappl G, Tilgen W, et al. Increased serum concentration of angiogenic factors in malignant melanoma patients correlates with tumor progression and survival. *J Clin Oncol*. 2001;19(2):577–583. doi: [10.1200/JCO.2001.19.2.577](https://doi.org/10.1200/JCO.2001.19.2.577)
- [34] Ding G, Chen X, Zhu J, et al. Identification of two aberrant transcripts derived from a hybridoma with amplification of functional immunoglobulin variable genes. *Cell Mol Immunol*. 2010;7(5):349–354. doi: [10.1038/cmi.2010.33](https://doi.org/10.1038/cmi.2010.33)
- [35] Bradbury ARM, Trinklein ND, Thie H, et al. When monoclonal antibodies are not monospecific: Hybridomas frequently express additional functional variable regions. *MAbs*. 2018;10(4):539–546. doi: [10.1080/19420862.2018.1445456](https://doi.org/10.1080/19420862.2018.1445456)
- [36] Zhu Z, Dimitrov DS. Construction of a large naïve human phage-displayed fab library through one-step cloning. *Methods Mol Biol*. 2009;525:1–12.
- [37] Kabat EA, Wu TT, Perry HM, et al. Sequences of proteins of immunological interest. 5th ed. Bethesda, MD: U.S. Dept. of Health and Human Services, Public Health Service, National Institutes of Health; 1991.
- [38] Tsuruta LR, Tomioka Y, Hishinuma T, et al. Characterization of 11-dehydro-thromboxane B2 recombinant antibody obtained by phage display technology. *Prostaglandins Leukot Essent Fatty Acids*. 2003;68(4):273–284. doi: [10.1016/S0952-3278\(03\)00006-1](https://doi.org/10.1016/S0952-3278(03)00006-1)
- [39] Murata VM, Schmidt MCB, Kalil J, et al. Anti-digoxin fab variants generated by phage display. *Mol Biotechnol*. 2013;54(2):269–277. doi: [10.1007/s12033-012-9564-1](https://doi.org/10.1007/s12033-012-9564-1)
- [40] Oliveira MLS, Coutinho JA, Krieger JE, et al. Site-directed mutagenesis of bovine FGF-2 cDNA allows the production of the human-form of FGF-2 in *Escherichia coli*. *Biotechnol Lett*. 2001;23(14):1151–1157. doi: [10.1023/A:1010528404170](https://doi.org/10.1023/A:1010528404170)
- [41] Xia J, Zhang Y, Qian J, et al. Isolation, identification and expression of specific human CD133 antibodies. *Sci Rep*. 2013;3(1):1–9. doi: [10.1038/srep03320](https://doi.org/10.1038/srep03320)
- [42] Andris-Widhopf J, Rader C, Steinberger P, et al. Methods for the generation of chicken monoclonal antibody fragments by phage display. *J Immunol Methods*. 2000;242(1–2):159–181. doi: [10.1016/S0022-1759\(00\)00221-0](https://doi.org/10.1016/S0022-1759(00)00221-0)
- [43] Green M, Sambrook J. *Molecular cloning: A laboratory manual*. 4th. New York, USA: Cold Spring Harbor Laboratory Press; 2012.
- [44] Wardemann H, Kofer J. Expression cloning of human B cell immunoglobulins. *Methods Mol Biol*. 2013;971:93–111.
- [45] Leem J, Dunbar J, Georges G, et al. ABodyBuilder: Automated antibody structure prediction with data-driven accuracy estimation. *MAbs* [Internet]. 2016;8:1259–1268. Available from. doi: [10.1080/19420862.2016.1205773](https://doi.org/10.1080/19420862.2016.1205773)
- [46] Marks C, Nowak J, Klostermann S, et al. Sphinx: Merging knowledge-based and ab initio approaches to improve protein loop prediction. *Bioinformatics*. 2017;33(9):1346–1353. doi: [10.1093/bioinformatics/btw823](https://doi.org/10.1093/bioinformatics/btw823)
- [47] Van Zundert GCP, Rodrigues JPGLM, Trellet M, et al. The HADDOCK2.2 web server: User-friendly integrative modeling of biomolecular complexes. *J Mol Biol* [Internet]. 2016;428(4):720–725. Available from. doi: [10.1016/j.jmb.2015.09.014](https://doi.org/10.1016/j.jmb.2015.09.014)
- [48] Ambrosetti F, Jandova Z, Bonvin AMJJ. A protocol for information-driven antibody-antigen modelling with the HADDOCK2.4 webserver. *ArXiv* [Internet]. 2020;1–22. Available from: <http://arxiv.org/abs/2005.03283>.
- [49] Méndez R, Leplae R, Lensink MF, et al. Assessment of CAPRI predictions in rounds 3-5 shows progress in docking procedures. *Proteins: Structure, Function And Genetics*. 2005;60(2):150–169. doi: [10.1002/prot.20551](https://doi.org/10.1002/prot.20551)
- [50] Laskowski R, Swindells M. LigPlot+: multiple ligand-protein interaction diagrams for drug discovery. *J Chem Inf Model*. 2011;51(10):2778–2786. doi: [10.1021/ci200227u](https://doi.org/10.1021/ci200227u)
- [51] Venkataraman G, Raman R, Sasisekharan V, et al. Molecular characteristics of fibroblast growth factor-fibroblast growth factor receptor-heparin-like glycosaminoglycan complex. *Proc Natl Acad Sci U S A*. 1999;96(7):3658–3663. doi: [10.1073/pnas.96.7.3658](https://doi.org/10.1073/pnas.96.7.3658)
- [52] Ye S, Luo Y, Lu W, et al. Structural basis for interaction of FGF-1, FGF-2, and FGF-7 with different heparan sulfate motifs. *Biochemistry*. 2001;40(48):14429–14439. doi: [10.1021/bi011000u](https://doi.org/10.1021/bi011000u)
- [53] LI D, Wang H, Xiang J-J, et al. Monoclonal antibodies targeting basic fibroblast growth factor inhibit the growth of B16 melanoma in vivo and in vitro. *Oncol Rep*. 2010;24(2):457–463. doi: [10.3892/or_00000879](https://doi.org/10.3892/or_00000879)
- [54] Wang L, Park H, Chhim S, et al. A novel monoclonal antibody to fibroblast growth factor 2 effectively inhibits growth of hepatocellular carcinoma xenografts. *Mol Cancer Ther*. 2012;11(4):864–872. doi: [10.1158/1535-7163.MCT-11-0813](https://doi.org/10.1158/1535-7163.MCT-11-0813)
- [55] Yang Y, Luo Z, Qin Y, et al. Production of bFGF monoclonal antibody and its inhibition of metastasis in Lewis lung carcinoma. *Mol Med Rep*. 2017;16(4):4015–4021. doi: [10.3892/mmr.2017.7099](https://doi.org/10.3892/mmr.2017.7099)
- [56] Wang S, Qin Y, Wang Z, et al. Construction of a human monoclonal antibody against bFGF for suppression of NSCLC. *J Cancer*. 2018;9(11):2003–2011. doi: [10.7150/jca.24255](https://doi.org/10.7150/jca.24255)
- [57] Tao J, Xiang JJ, Li D, et al. Selection and characterization of a human neutralizing antibody to human fibroblast growth factor-2. *Biochem Biophys Res Commun*. 2010;394(3):767–773. doi: [10.1016/j.bbrc.2010.03.067](https://doi.org/10.1016/j.bbrc.2010.03.067)
- [58] Presta LG. Molecular engineering and design of therapeutic antibodies. *Curr Opin Immunol*. 2008;20(4):460–470. doi: [10.1016/j.coi.2008.06.012](https://doi.org/10.1016/j.coi.2008.06.012)

- [59] Mirick GR, Bradt BM, Denardo SJ, et al. A review of human anti-globulin antibody (HAGA, HAMA, HACA, HAHA) responses to monoclonal antibodies. Not four letter words. *Q J Nucl Med Mol Imaging*. 2004;48(4):251–257.
- [60] Carmen S, Jermutus L. Concepts in antibody phage display. *Brief Funct Genomic Proteomic*. 2002;1(2):189–203. doi: [10.1093/bfgp/1.2.189](https://doi.org/10.1093/bfgp/1.2.189)
- [61] Steinberger P, Sutton JK, Rader C, et al. Generation and characterization of a recombinant human CCR5-specific antibody. *J Biol Chem*. 2000;275(46):36073–36078. doi: [10.1074/jbc.M002765200](https://doi.org/10.1074/jbc.M002765200)
- [62] Boado RJ, Zhang Y, Zhang Y, et al. Humanization of anti-human Insulin receptor antibody for drug targeting across the human blood–brain barrier. *Biotechnol Bioeng*. 2007;96(2):381–391. doi: [10.1002/bit.21120](https://doi.org/10.1002/bit.21120)
- [63] Makabe K, Nakanishi T, Tsumoto K, et al. Thermodynamic consequences of mutations in vernier zone residues of a humanized anti-human epidermal growth factor receptor murine antibody, 528. *J Biol Chem*. 2008;283(2):1156–1166. doi: [10.1074/jbc.M706190200](https://doi.org/10.1074/jbc.M706190200)
- [64] Tsuiji M, Yurasov S, Velinzon K, et al. A checkpoint for autoreactivity in human IgM+ memory B cell development. *J Exp Med*. 2006;203(2):393–400. doi: [10.1084/jem.20052033](https://doi.org/10.1084/jem.20052033)
- [65] Eccles SA, Box C, Court W. Cell migration/invasion assays and their application in cancer drug discovery. *Biotechnol Annu Rev*. 2005;11:391–421.
- [66] Goodwin AM. In vitro assays of angiogenesis for assessment of angiogenic and anti-angiogenic agents. *Microvasc Res*. 2007;74(2–3):172–183. doi: [10.1016/j.mvr.2007.05.006](https://doi.org/10.1016/j.mvr.2007.05.006)
- [67] Cao L, Liu H, Lam DSC, et al. In vitro screening for angiostatic potential of herbal chemicals. *Invest Ophthalmol Vis Sci*. 2010;51(12):6658–6664. doi: [10.1167/iovs.10-5524](https://doi.org/10.1167/iovs.10-5524)
- [68] Friedl P, Wolf K. Tumour-cell invasion and migration: Diversity and escape mechanisms. *Nat Rev Cancer*. 2003;3(5):362–374. doi: [10.1038/nrc1075](https://doi.org/10.1038/nrc1075)
- [69] Xu L, Gordon R, Farmer R, et al. Structural absorption by barbule microstructures of super black bird of paradise feathers. *Nat Commun*. 2018;9(1):1–14. doi: [10.1038/s41467-017-02088-w](https://doi.org/10.1038/s41467-017-02088-w)
- [70] de Aguiar RB, da Silva TDA, Costa BA, et al. Generation and functional characterization of a single-chain variable fragment (scFv) of the anti-FGF2 3F12E7 monoclonal antibody. *Sci Rep*. 2021;11(1):1–11. doi: [10.1038/s41598-020-80746-8](https://doi.org/10.1038/s41598-020-80746-8)
- [71] Xie Y, Su N, Yang J, et al. FGF/FGFR signaling in health and disease. *Sig Transduct Target Ther*. 2020;5(1):181. doi: [10.1038/s41392-020-00222-7](https://doi.org/10.1038/s41392-020-00222-7)